

**AD-A263 570**

A standard linear barcode is located in the top left corner of the page.

**CUMENTATION PAGE**

Form Approved  
OMB No. 0704-0128

2

Comments are invited to the Director of the Office of Information and Records, 215 Jefferson, concerning the burden of preparing and reviewing the following information and comments regarding this burden estimate in the preparation of this request for this agency's burden to the Director of Headquarters Services, Directorate for Information Operations and Reports, 302, and to the Office of Management and Budget, Paperwork Reduction Project 0704-0188, Washington, DC 20540.

		2. REPORT DATE April 20, 1993	3. REPORT TYPE AND DATES COVERED Reprint
4. TITLE AND SUBTITLE  Modeling the Bidirectional Reflectance and Spectral Albedo of a Conifer Forest		5. FUNDING NUMBERS  PE62101F PR 6670 TA GP WU 12	
6. AUTHOR(S)  Crystal Barker Schaaf, Alan H. Strahler *			
7. PERFORMING ORGANIZATION NAME(S) AND ADDRESS(E)  Phillips Lab/GPAA 29 Randolph Road Hanscom AFB, MA 01731-3010		8. PERFORMING ORGANIZATION REPORT NUMBER  PL-TR-93-2096	
9. SPONSORING/MONITORING AGENCY NAME(S) AND ADDRESS(E)  SAR 29 APR 1993 S B D		10. SPONSORING MONITORING AGENCY REPORT NUMBER	
11. SUPPLEMENTARY NOTES * Center for Remote Sensing, Boston University, 725 Commonwealth Ave, Boston MA 02215 Presented at the 25th International Symposium, Remote Sensing and Global Environmental Change, Graz, Austria, 4-8 April 1993			
12a. DISTRIBUTION/AVAILABILITY STATEMENT  Approved for public release; Distribution unlimited		12b. DISTRIBUTION CODE	
13. ABSTRACT (Maximum 200 words)  Analysis of aircraft imagery and ground measurements acquired for a spruce forest stand in Howland, Maine as part of the 1990 Forest Ecosystem Dynamics Multisensor Aircraft Campaign (FEDMAC), show that the Li-Strahler geometric-optical forest canopy reflectance model can estimate spectral bidirectional reflectance factors and spectral albedo with some success. In this model, the vegetated surface is treated as an assemblage of partially illuminated tree crowns of ellipsoidal shape, and through geometric-optics and Boolean set theory, the proportion of sunlit and shadowed canopy and background is modeled as a function of view angle. The model is driven by ground measurements of spectral reflectance and tree crown shape, size and spacing. Atmospherically corrected multiangular radiance measurements from the Advanced Solid State Array Spectroradiometer (ASAS) fit the shape of the modeled reflectance function quite well. Integration of the reflectance function yields a spectral albedo, which, when extended to the full solar spectrum, agrees with pyranometer measurements obtained at the site.			
14. SUBJECT TERMS Albedo, Hemispherical reflectance, Bidirectional reflectance, Canopy modeling, Surface reflectance modeling			15. NUMBER OF PAGES 8
			16. PRICE CODE
17. SECURITY CLASSIFICATION OF REPORT UNCLASSIFIED	18. SECURITY CLASSIFICATION OF THIS PAGE UNCLASSIFIED	19. SECURITY CLASSIFICATION OF ABSTRACT UNCLASSIFIED	20. LIMITATION OF ABSTRACT SAR

## MODELING THE BIDIRECTIONAL REFLECTANCE AND SPECTRAL ALBEDO OF A CONIFER FOREST\*

Crystal Barker Schaaf

Geophysics Directorate, Phillips Lab,  
29 Randolph Rd, Hanscom AFB, MA 01731, USA

Alan H. Strahler

Center for Remote Sensing, Boston University,  
725 Commonwealth Ave, Boston, MA 02215, USA

### ABSTRACT

Analysis of aircraft imagery and ground measurements acquired for a spruce forest stand in Howland, Maine as part of the 1990 Forest Ecosystem Dynamics Multisensor Aircraft Campaign (FEDMAC), show that the Li-Strahler geometric-optical forest canopy reflectance model can estimate spectral bidirectional reflectance factors and spectral albedo with some success. In this model, the vegetated surface is treated as an assemblage of partially illuminated tree crowns of ellipsoidal shape, and through geometric-optics and Boolean set theory, the proportion of sunlit and shadowed canopy and background is modeled as a function of view angle. The model is driven by ground measurements of spectral reflectance and tree crown shape, size and spacing. Atmospherically corrected multiangular radiance measurements from the Advanced Solid State Array Spectroradiometer (ASAS) fit the shape of the modeled reflectance function quite well. Integration of the reflectance function yields a spectral albedo, which, when extended to the full solar spectrum, agrees with pyranometer measurements obtained at the site.

### 1.0 INTRODUCTION

The anisotropy exhibited by forest canopies is determined by the canopy structure, shape and density, shadowing patterns, multiple scattering interactions within the canopy, leaf angle distributions and the specularity of the foliage. Although dense, uniform canopies have primarily been modeled with homogeneous plane-parallel or three-dimensional radiative transfer models (Verhoef, 1984; Gerstl and Simmer, 1986; Kimes *et al.*, 1987; Kimes, 1984; 1991; Nilson and Kuusk, 1989; Myneni *et al.*, 1989; Verstraete *et al.*, 1990), simpler geometric-optical models have shown some success in modeling non-uniform and particularly sparse forests (Li and Strahler, 1985; 1986; 1992a; b; Strahler and Jupp, 1990a; b; Abuelgasim and Strahler, 1993). Because sparse canopies, or forests with significant height variations produce complex shadowing patterns, the interplay between the sunlit and shadowed components of the canopy is the primary determiner of the radiation reflected.

The Li-Strahler geometric-optical model exploits these shadowing effects by modeling a scene or pixel as an assemblage of ellipsoidal tree crowns. Geometric-optics and Boolean set theory are used to determine the areal proportions of shadowed and sunlit canopy and shadowed and sunlit background associated with a solar zenith angle. Independent characteristic signatures for each component are weighted by these areal proportions and used to determine the spectral directional reflectance factor of the canopy at any viewing angle. Although these component signatures do not include an explicit treatment of diffuse irradiance, canopy multiple scattering or leaf specularity and are applied uniformly to the areal proportions, they are reasonable approximations for clear atmospheres and low to medium solar zenith angles. The geometric-optical model does incorporate the effects of mutual shadowing or the obscuring of tree crowns by one another and takes into account the impact bright unshadowed tree tips have on the canopy reflectance at very high view angles. By performing a hemispherical integration, the model also provides an instantaneous hemispherical reflectance (or spectral surface albedo).

\*Presented at the 25th International Symposium, Remote Sensing and Global Environmental Change, Graz, Austria, 4-8 April 1993.

93-09123



93

The availability of directional radiances from the Advanced Solid State Array Spectroradiometer (ASAS) obtained during the 1990 Forest Ecosystem Dynamics Multisensor Aircraft Campaign (FED-MAC) in Howland, Maine makes a validation of the model possible. Atmospherically-corrected ASAS reflectances are typically obtained in at least the principal plane and cross-principal plane of the sun. They can be compared (both in shape and magnitude) to modeled bidirectional reflectance factors (BRFs) when the model has been carefully calibrated with accurate tree shape measurements and component signatures measured in the field at the time of the ASAS overpass. Although sky radiance, multiple scattering and specular effects are not explicitly incorporated in the Li-Strahler model, they are implicit in the field-measured component signatures.

In addition to validating the model BRFs, the spectral hemispherical reflectances computed by the geometric-optical model can be combined (Brest and Goward, 1987; Brest, 1987) to produce a surface albedo that can be validated with pyranometer measurements obtained on the site at the overpass times.

## 2.0 PROCEDURE

### 2.1 ASAS IMAGES

At 9:12 EDST, 8 Sept 1990, the ASAS instrument was flown on a NASA C-130 aircraft at 4603 meters altitude in the principal plane of the sun over the FEDMAC spruce site. This site is in the vicinity of an instrumented meteorological tower maintained by the University of Maine at Orono ( $45^{\circ} 21.21'N$ ,  $68^{\circ} 44.49'W$ ). ASAS images are obtained at seven look angles from  $+45^{\circ}$  to  $-45^{\circ}$ . The red band 15 (band center 644.6 nm) and near-infrared band 24 (band center 773.5 nm) were selected for this study. A fairly uniform region of vegetation was selected around the tower and the mean brightness for this area was obtained from each image. This brightness was then transformed to radiance with the NASA-provided radiometric resolution factors. Finally the values were atmospherically corrected using the Liang and Strahler (1992) model as parameterized by aerosol optical depths measured on the site at the time of the overpass. The cross-principal plane images were obtained somewhat later at 9:40 EDST and subjected to the same processing.

### 2.2 FOREST CHARACTERISTICS

In 1989 investigators from Boston University surveyed the spruce stand near the tower, and used variable radius plot sampling (Dilworth, 1977) to obtain tree height, diameter-at-breast height, crown width, and height-to-crown distance. These data were supplemented with tree heights collected by University of Virginia researchers. Based on the sample of 40 trees, the parameters used as input to the geometric-optical model were basal-area-weighted means of height-to-center-of-crown ( $9.9 \pm 2.4m$ ), crown radius (2.2m), crown vertical radius (3.6m), and density (1161 trees/hectare).

In 1990, at the time of the ASAS overpass, radiances were collected using a handheld radiometer (Spectron Engineering SE590) for use as the sunlit and shadowed component signatures required by the model. Bands 97 (643.7 nm) and 141 (774.1 nm) were used to match the band centers of the ASAS channels. Sunlit and shadowed crown measurements were taken within half an hour of the overpass time. Spectralon panel measurements were also taken so that reflectance factors could be computed. The shadowed and sunlit background signatures were composites of radiances from litter, ferns, shrubs, moss and grasses. Unfortunately, the background signatures were measured about 2 hours after the overpass. However, given the fairly large solar zenith angle ( $58.79^{\circ}$ ) and the high density and crown coverage (84%), the crown components would be the primary contributors to the scene reflectance rather than the background components. So, the later background signatures were used (with no attempt to correct for solar zenith angle). A three-component version of the model was used, so that the shadowed component is the average of the background and canopy signatures. The final component signatures used in the model for the red spectral region were a sunlit canopy of 0.0349, a sunlit background of 0.0503, and shadows of 0.0017. For the NIR spectral region values used were a sunlit canopy of 0.3969, a sunlit background of 0.3248, and shadows of 0.0375.

DTIC

1985 Code  
FBI and/or  
Dist. special

A-1

## 2.3 ALBEDOS

Upward and downward pointing Eppley PSP pyranometers were positioned at a height of 25.8 meters on a boom extending 2.4m west of the meteorological tower at the spruce site. These data can be ratioed to produce instantaneous full-spectrum surface albedos (.3-3 $\mu$ m). During the times of the ASAS overpasses, these surface albedos range from 0.117 to 0.111.

## 3.0 RESULTS

### 3.1 MODEL VERSUS ASAS REFLECTANCES

Using the forest characteristics, the component signatures, and the appropriate solar zenith angle, the geometric-optical model was used to simulate the spruce site at the time of the ASAS overpass. The red and NIR bidirectional reflectance distribution functions (BRDFs) are displayed in Figure 1. The three dimensional BRDFs are displayed in a rectangular coordinate system where each view angle in the hemisphere is taken as a pair of polar coordinates and transformed onto the x-y plane as a vector of unit length. The corresponding reflectances are then plotted along the z axis. The hotspot occurs where the viewing angle and solar zenith angle coincide thus concealing shadows. The bowl occurs when the view angle moves opposite the solar zenith angle and more and more of the shadows are revealed. The width of the hotspot is governed by the elliptical shape of the crowns. The shape of the bowl is governed by the density of the forest and the amount of mutual shadowing that is taking place. By extracting results along the principal plane, the modeled near-infrared BRFs can be compared to the ASAS BRFs (Figure 2). The model predicts brighter values in the forward scattering directions than were detected by the ASAS imagery. However, the general shape and magnitude were quite good. The modeling was repeated with the same component signatures but with the solar zenith angle that corresponded to the cross-principal plane flight (54.54°). In the cross-principal plane direction (Figure 3), the model overestimates the impact of the mutual shadowing by creating more of a valley shape than the shallow bowl shape revealed by the ASAS imagery. However, the magnitude is quite reasonable.

### 3.2 MODEL ALBEDO VERSUS MEASURED ALBEDO

An integration over the viewing hemispheres of Figure 1 result in a spectral hemispherical reflectance or surface albedo. Brest and Goward (1987) suggest that the red spectral model albedo is representative of a 0.526 proportion, that the near-infrared model albedo is representative of a 0.362 proportion and the mid-infrared is representative of a 0.112 proportion of solar radiation incident at the surface. Therefore, red, near-infrared, and mid-infrared spectral albedos can be weighted by these proportions and added to estimate the broadband value. Since there were no mid-infrared radiometer measurements made to use as component signatures, no mid-infrared model runs could be made. However, Brest and Goward (1987) use 0.5 of the near-infrared value as an appropriate approximation of the mid-infrared value. Using these assumptions, full spectrum model surface albedos can be computed and compared with the pyranometer measurements taken at the site. The geometric-optical model produced values of 0.1025 and 0.1102 at the times of the ASAS overpasses, while the pyranometer measured values during that time range from 0.117 to 0.111 (Figure 4). These model values were quite close in magnitude to the measured values.

## 4.0 CONCLUSIONS

The Li-Strahler geometric-optical model was validated with data collected from a spruce forest in Maine during the 1990 FEDMAC data collection effort. Although modeled near-infrared BRFs agreed quite well with ASAS reflectances along the principal plane in both shape and magnitude, a comparison of the cross-principal plane values reveal that the model tends to overestimate the reflectance at mid-to-high viewing angles by slightly overemphasizing the impact of mutual shadowing. Model spectral albedos were combined to produce full spectrum albedos that could be compared with pyranometer measurements taken at the site at the same time as the ASAS overpasses. Given the simplicity of the model

and the difficulties in obtaining realistic and timely component signatures, the close agreement found between the measurements and model results is quite encouraging.

Such success demonstrates the adaptability of the geometric-optical model but also highlights its dependence on accurate and timely sunlit and shadowed component signatures. Work is underway to produce a hybrid model that treats canopy scattering as a function of path length and gap probability (Li and Strahler, 1988; Strahler and Jupp, 1990) and combines the scattering with the geometric-optical effects of the trees within the canopy. Such efforts will result in a model that obviates component signatures and does not suffer from a sensitivity to site and time specific spectral measurements.

#### ACKNOWLEDGEMENTS

The authors would like to thank Abdelgadir Abuelgasim for his assistance in preparing the ASAS data and the model inputs, Dr Shunlin Liang for the use of his atmospheric correction model and Dr Xiaowen Li for his helpful suggestions in using the geometric-optical model. The forest characteristics field data collection was supported by NASA grant NAGW-2082. The efforts of the second author were also partially supported by this grant as well as NASA contract NAS5-31369. ASAS, pyranometer, and aerosol optical depth data were provided by the FED project. We thank Drs Jon Ranson and Jim Irons of NASA/GSFC for their assistance with the FEDMAC data set and the ASAS imagery.

#### REFERENCES

Abuelgasim, A., and Strahler, A.H., 1993: Modeling bidirectional radiance measurements collected by the Advanced Solid-state Array Spectroradiometer over Oregon Transect conifer forest. accepted *Remote Sens. Environ.*.

Brest, C.L., and Goward, S.N., 1987: Deriving surface albedo measurements from narrowband satellite data. *Int J. Remote Sensing*, **8**, 351-367.

Brest, C.L., 1987: Seasonal albedo of an urban/rural landscape from satellite observations. *J. Clim. Appl. Meteor.*, **26**, 1169-1187.

Dilworth, J., 1977: *Log scaling and timber cruising*. O.S.U. Book Stores, Inc., Corvalis, Oregon.

Gerstl, S.A.W., and Borel, C.C.: Principles of the radiosity method versus radiative transfer for canopy reflectance modeling. *IEEE Trans. Geosci. Remote Sensing*, **30**, 271-275.

Kimes, D.S., 1991: Radiative transfer in homogeneous and heterogeneous vegetation canopies. *Photo-vegetation interactions*, ed. Myneni and Ross, Springer-Verlag, Berlin, 339-388.

Kimes, D. S., 1984: Modeling the directional reflectance form complete homogeneous vegetation canopies with various leaf-orientation distributions. *J. Opt. Soc. Am.*, **1**, 725-737.

D. S. Kimes, P. J. Sellers, and W. W. Newcomb, 1987: Hemispherical Reflectance Variations of Vegetation Canopies and Implications for Global and Regional Energy Budget Studies, *J. Clim. Appl. Meteor.*, **26**, 959-972.

Li, X., and Strahler, A.H., 1992a: Geometric-optical bidirectional reflectance modeling of the discrete-crown vegetation canopy: Effect of crown shape and mutual shadowing. *IEEE Trans. Geosci. Remote Sensing*, **30**, 276-292.

Li, X., and Strahler, A.H., 1992b: Mutual shadowing and directional reflectance of a rough surface: A geometric-optical model. *Proceedings, International Geosciences and Remote Sensing Symposium*.

um: *IGARSS92*, Houston, TX, 766-768.

Li, X., and Strahler, A. H., 1988: Modeling the gap probability of a discontinuous vegetation canopy. *IEEE Trans. Geosci. Remote Sensing*, **26**, 161-170.

Li, X., and Strahler, A. H., 1986: Geometric-optical bidirectional reflectance modeling of a conifer forest canopy. *IEEE Trans. Geo. Rem. Sens.*, **GE-24**, 906-919.

Li, X., and Strahler, A. H., 1985: Geometric-optical modeling of a conifer forest. *IEEE Trans. Geo. Rem. Sens.*, **GE-23**, 705-721.

Liang, S., and Strahler, A. H., 1993: Retrieval of surface BRDF and albedo from multiangle remotely sensed data. submitted *Remote Sens. Environ.*.

Myneni, R.B., Ross, J., and Asrar, G., 1989: A review on the theory of photon transport in leaf canopies. *Agric Forest Meteor*, **45**, 165pp.

Nilson, T., and Kuusk, A., 1989: A reflectance model for the homogeneous plant canopy and its inversion. *Remote Sens. Environ.*, **27**, 157-167.

Strahler, A. H., and Jupp, D. L. B., 1990a: Bidirectional reflectance modeling of forest canopies using boolean models and geometric optics. *Proceedings, International Geosciences and Remote Sensing Symposium:IGARSS90*, Washington DC.

Strahler, A. H., and Jupp, D. L. B., 1990b: Modeling bidirectional reflectance of forests and woodlands using boolean models and geometric optics. *Remote Sens. Environ.*, **34**, 153-166.

Verhoef, W., 1984: Light scattering by leaf layers with application to canopy reflectance modeling: The SAIL model. *Remote Sens. Environ.*, **16**, 125-141.

Verstraete, M., Pinty, B., and Dickinson, R.E., 1990: A physical model of the bidirectional reflectance of vegetation canopies: I Theory. *J. G. R.*, **95-D8**, 11755-11765.

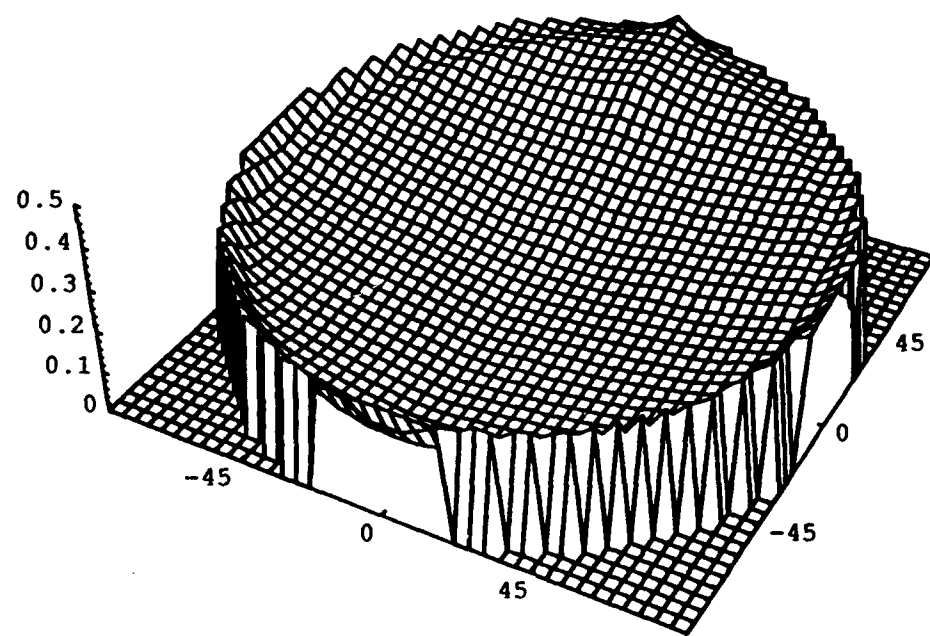
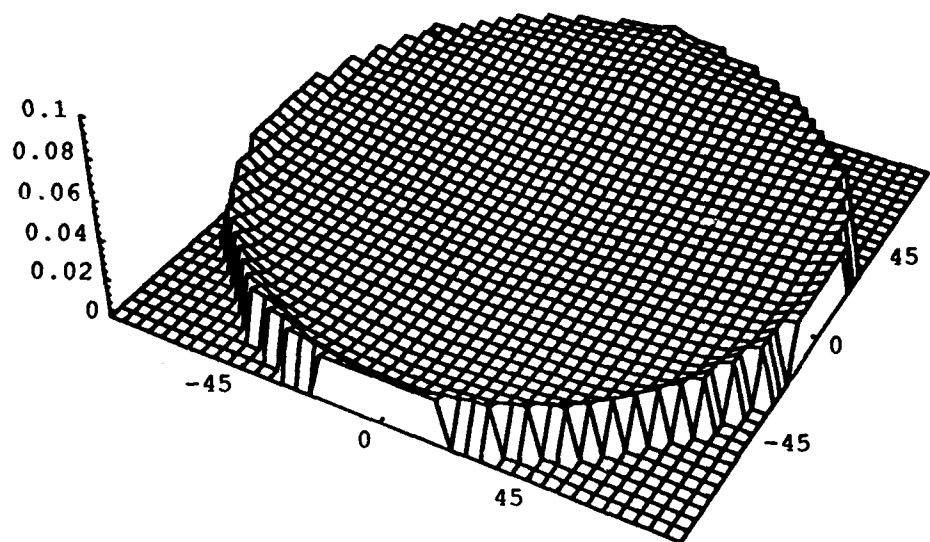


**Figure 1.** Red and NIR geometric-optical model bidirectional reflectance distribution functions at the time of the ASAS principal plane overpass (SZN 58.79 °, GMT 13:12)

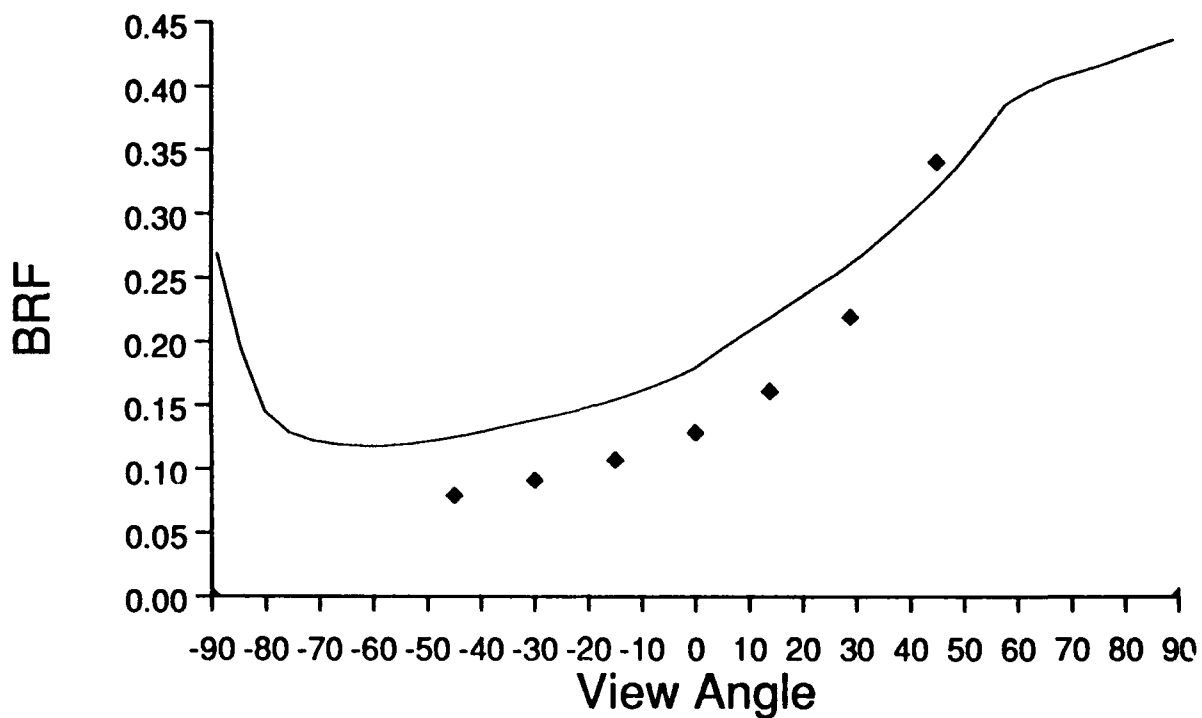


Figure 2. Mean NIR ASAS Reflectances (◆) Compared With The Modeled BRFs (—) Along The Principal Plane (SZN 58.79 °, GMT 13:12).

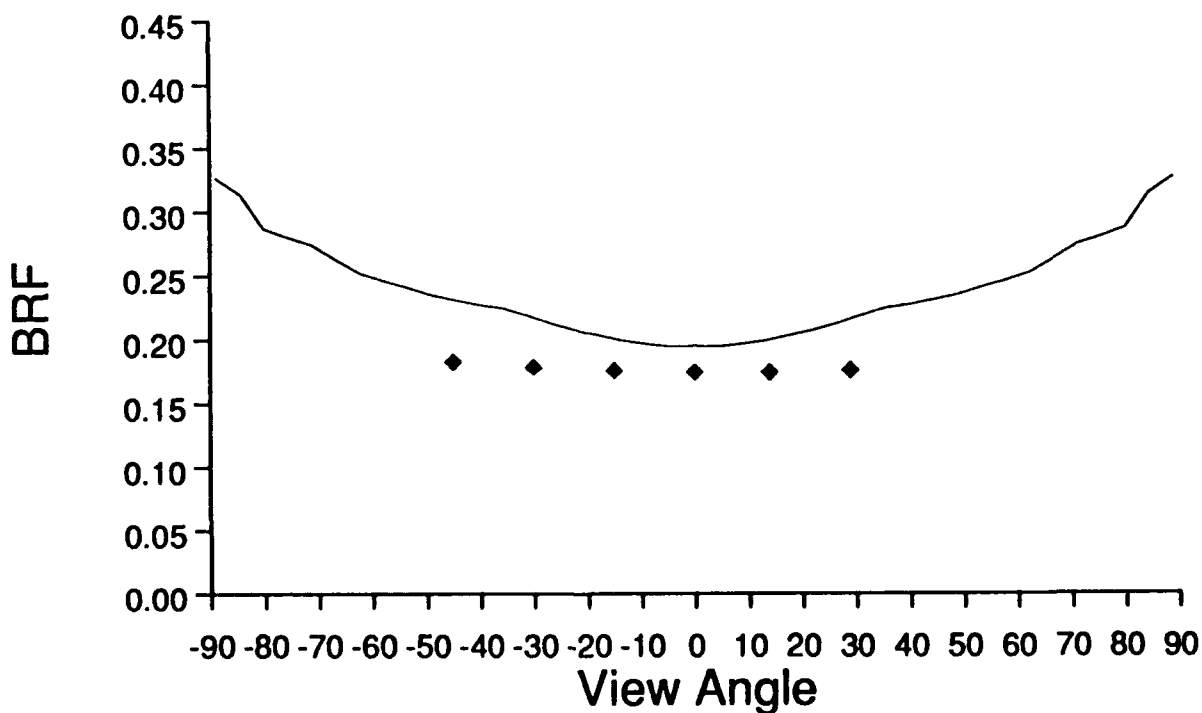


Figure 3. Mean NIR ASAS Reflectances (◆) Compared With The Modeled BRFs (—) Along The Cross-Principal Plane (SZN 54.54 °, GMT 13:40).

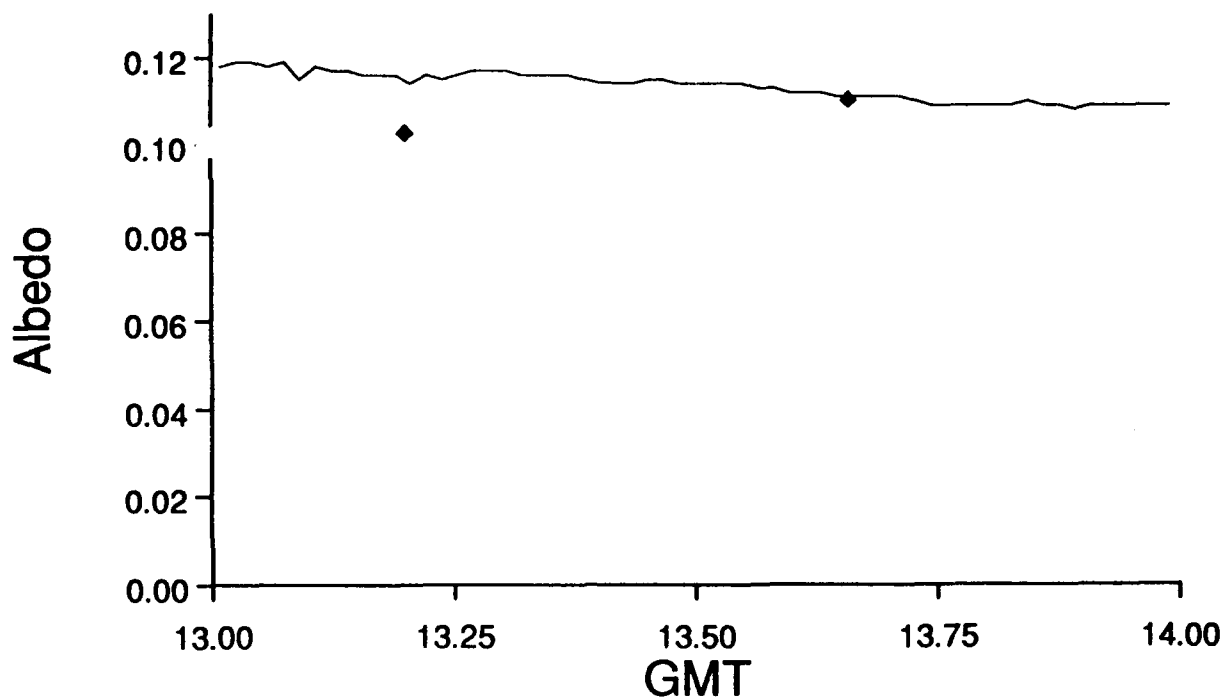


Figure 4. Measured (♦) and Modeled (→) Surface Albedos at ASAS Overpass Times.